

1-1-2004

Western Pacific coral delta18O records of anomalous Holocene variability in El Nino-Southern Oscillation

Helen V. McGregor
University of Wollongong, mcgregor@uow.edu.au

M Gagan

Follow this and additional works at: <https://ro.uow.edu.au/scipapers>



Part of the [Life Sciences Commons](#), [Physical Sciences and Mathematics Commons](#), and the [Social and Behavioral Sciences Commons](#)

Recommended Citation

McGregor, Helen V. and Gagan, M: Western Pacific coral delta18O records of anomalous Holocene variability in El Nino-Southern Oscillation 2004.
<https://ro.uow.edu.au/scipapers/4235>

Western Pacific coral delta18O records of anomalous Holocene variability in El Nino-Southern Oscillation

Keywords

delta18o, variability, el, nino, southern, oscillation, western, pacific, coral, records, anomalous, holocene, GeoQUEST

Disciplines

Life Sciences | Physical Sciences and Mathematics | Social and Behavioral Sciences

Publication Details

McGregor, H. V. & Gagan, M. (2004). Western Pacific coral delta18O records of anomalous Holocene variability in El Nino-Southern Oscillation. *Geophysical Research Letters*, 31 (L11204), L11204-1-L11204-4.

Western Pacific coral $\delta^{18}\text{O}$ records of anomalous Holocene variability in the El Niño–Southern Oscillation

Helen V. McGregor and Michael K. Gagan

Research School of Earth Sciences, The Australian National University, Canberra, Australia

Received 12 March 2004; accepted 18 May 2004; published 15 June 2004.

[1] Skeletal oxygen isotope ratios in Holocene *Porites* corals from northern Papua New Guinea record decreases in sea surface temperature (SST) and rainfall during El Niño events. Threshold analysis of seven fossil coral $\delta^{18}\text{O}$ records spanning the period 7.6–5.4 ka (thousand years ago) shows 8–12 El Niño events/century, significantly less than the 23 events/century recorded by the NINO3.4 Index. The coral reconstructions also show a 15% reduction in El Niño event amplitude for 7.6–5.4 ka, compared to today, which is greater than the suppression given by model studies. In contrast, large and protracted El Niño events are identified for 2.5–1.7 ka. Taken together, the results indicate a non-linear atmospheric response to Holocene changes in El Niño SST anomalies. We propose that small changes in tropical SST gradients, the positioning of the Intertropical Convergence Zone, and the Pacific tradewind climatology modify the impact of El Niño events on western Pacific rainfall. **INDEX TERMS:** 1620 Global Change: Climate dynamics (3309); 4522 Oceanography: Physical: El Niño; 4870 Oceanography: Biological and Chemical: Stable isotopes; 9355 Information Related to Geographic Region: Pacific Ocean. **Citation:** McGregor, H. V., and M. K. Gagan (2004), Western Pacific coral $\delta^{18}\text{O}$ records of anomalous Holocene variability in the El Niño–Southern Oscillation, *Geophys. Res. Lett.*, 31, L11204, doi:10.1029/2004GL019972.

1. Introduction

[2] Model results for the early-middle Holocene (11–4 ka) suggest that ocean-atmosphere feedbacks in response to changes in the Earth's orbital parameters increase the east-west SST gradient across the Pacific, leading to suppression of El Niño events [Clement *et al.*, 2000]. This conclusion is broadly supported by a variety of paleo-data from the tropical Pacific region [Shulmeister and Lees, 1995; Rodbell *et al.*, 1999; Sandweiss *et al.*, 2001; Tudhope *et al.*, 2001; Moy *et al.*, 2002; Woodroffe *et al.*, 2003]. However, the magnitudes of changes in reconstructed and modeled El Niño–Southern Oscillation (ENSO) events differ significantly [Gagan *et al.*, 2004]. For example, the coupled ocean-atmosphere response to El Niño recorded by skeletal oxygen isotope ratios ($\delta^{18}\text{O}$) in fossil corals is larger than the modeled changes in El Niño SST anomalies [Clement *et al.*, 2000; Liu *et al.*, 2000; Woodroffe *et al.*, 2003]. Fossil coral records of ENSO are still rare, however, and additional reconstructions are necessary to understand the processes controlling the Holocene ENSO, and proxy-model discrepancies.

[3] Here, we use eight annually-resolved fossil coral $\delta^{18}\text{O}$ records from northern Papua New Guinea (PNG), near the core of the ENSO-sensitive Western Pacific Warm Pool, to investigate paleo-ENSO events during the middle to late Holocene. The fossil *Porites* used in this study were sampled during Leg 6b (May–June 1998) of Project TROPICS (Tropical River–Ocean Processes In Coastal Settings). A significant advantage of the multiple coral cores is that uncertainties in the paleo-ENSO reconstructions can be quantified.

2. Methods

[4] Fossil corals were drilled along their major growth axes in growth position from uplifted reefs on Koil Island and Muschu Island, offshore of the Sepik River, northern PNG (auxiliary Figure 1¹). Analogous modern corals were drilled from nearby reefs. Fossil corals were screened for diagenesis using X-ray diffraction and petrographic analysis [McGregor and Gagan, 2003]. Eight mid-late Holocene fossil corals were selected for study due to their well preserved state. Uranium-series ages of these corals were determined by isotope dilution thermal ionisation mass spectrometry, with fossil coral initial $\delta^{234}\text{U}$ constrained to 146–150‰. The average error on the uranium-series ages is ± 90 yr (2σ ; see auxiliary Table 1¹).

[5] Annual growth increments were milled from the modern and fossil corals, with divisions between climatological years defined by the transition from high to low density bands (\sim January), as shown by coral X-rays [McGregor, 2003] (auxiliary Figure 2¹). Oxygen isotope ratios were measured as outlined by McGregor and Gagan [2003]. Replicate aliquots of each annual sample were measured for $\delta^{18}\text{O}$ until the standard error of the mean $\delta^{18}\text{O}$ value fell below 0.05‰ to ensure that even subtle changes in coral $\delta^{18}\text{O}$ could be accurately discerned.

3. Modern ENSO Variability

[6] A modern *Porites lutea* coral from Muschu Island (MS01, identified by J. Veron, 2002), was analysed for $\delta^{18}\text{O}$ over the period 1910–1997. The reproducibility of the modern coral $\delta^{18}\text{O}$ signal was checked for the period 1983–1997 by analysing another *Porites lutea* from Muschu Island (MS04) and a *Porites sp.* from Koil Island (KL03, Figure 1 inset). The mean $\delta^{18}\text{O}$ values for the three modern corals are in good agreement ($-5.45 \pm 0.05\text{‰}$, 1σ) and the records show similar interannual variability. The

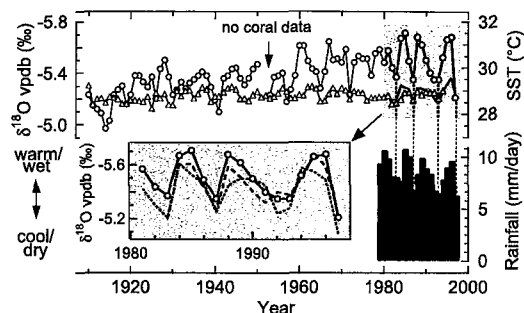


Figure 1. Comparison of modern Muschu Island (MS01) annual coral $\delta^{18}\text{O}$ (circles), CMAP Precipitation, and GOSTA (triangles) and IGOSS SST (solid line) records. Inset shows good reproducibility of the modern Muschu Island (MS01, line with circles; MS04, dashed line), and Koil Island (KL03; dotted line) coral $\delta^{18}\text{O}$ records for 1983–1997. The GOSTA and IGOSS SST records are for the 1° grid square centred on 03.5°S , 143.5°E , including the study area. The CMAP record is for the 2.5° grid square centred on 143°E , 1.25°S . Instrumental data were averaged to annual intervals to match the coral data. The $\delta^{18}\text{O}$ and SST axes are scaled using the relationship of Gagan *et al.* [1998]. The departure of the coral $\delta^{18}\text{O}$ record from the GOSTA SST during the later half of the 20th century highlights the dominance of changes in $\delta^{18}\text{O}_w$ (salinity) in controlling coral $\delta^{18}\text{O}$.

correlation coefficient (r) is 0.92 ($p > 0.001$) for the MS01 and MS04 $\delta^{18}\text{O}$ records and 0.86 ($p > 0.001$) for MS01 and KL03. We attribute the small differences in $\delta^{18}\text{O}$ between the three coral records to differences in the $\delta^{18}\text{O}$ of seawater ($\delta^{18}\text{O}_w$), rather than SST, as gradients in $\delta^{18}\text{O}_w$ between these sites are significant [McGregor, 2003].

[7] The good agreement of the coral $\delta^{18}\text{O}$ records indicates they are recording regional environmental signals. Interannual variability in the MS01 coral $\delta^{18}\text{O}$ for 1910–1997 is clearly dominated by changes in $\delta^{18}\text{O}_w$ because SSTs reconstructed from the coral $\delta^{18}\text{O}$ span 5°C [Gagan *et al.*, 1998], while the GOSTA SST range is only 1°C (Figure 1). Comparison of local SSTs and rainfall with the coral $\delta^{18}\text{O}$ record shows that $\delta^{18}\text{O}$ increases when SST and rainfall decrease during El Niño events [McPhaden and Picaut, 1990]. The coupling of changes in SST and the amount of ^{18}O -depleted rainfall in the tropical western Pacific makes the Muschu coral $\delta^{18}\text{O}$ a particularly sensitive recorder of ENSO variability. Increases in the $\delta^{18}\text{O}$ of Muschu Island seawater during El Niños are further enhanced through the movement of relatively saline ^{18}O -enriched thermocline water towards the surface [Tourre and White, 1997] and reduced runoff from the nearby Sepik River, which responds to ENSO-induced droughts in the PNG highlands [Ayliffe *et al.*, 2004].

[8] We tested the ability of Muschu coral $\delta^{18}\text{O}$ to record El Niños by comparing interannual $\delta^{18}\text{O}$ anomalies (defined as departures from the 10-year running mean) with the Southern Oscillation Index (SOI) and the NINO3.4 SST Index for 1910–1997 (Figure 2). The positive coral $\delta^{18}\text{O}$ anomalies record 14 out of 16 (88%) El Niño events (the 1963 and 1969 events are not recorded). The strength of the correlation coefficients (r) are similar for SOI vs NINO3.4 (-0.85 , $p > 0.001$) and coral $\delta^{18}\text{O}$ vs NINO3.4 (0.71 , $p >$

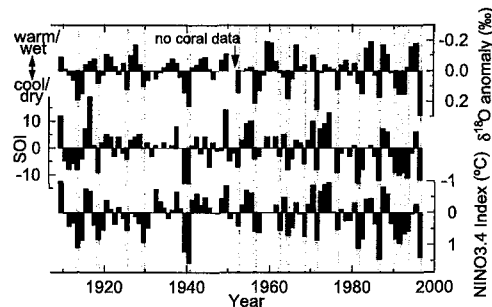


Figure 2. Comparison of modern coral MS01 annual $\delta^{18}\text{O}$ anomalies, the SOI, and the NINO3.4 Index. Annual coral $\delta^{18}\text{O}$ anomalies were calculated relative to a 10-year running mean. El Niño years for 1910–1997 (grey bars) are based on those of Trenberth [1997].

0.001). Importantly, the coral record does not indicate any positive $\delta^{18}\text{O}$ anomaly that is not linked to an El Niño event.

4. Mid-Holocene ENSO Variability

[9] The fossil coral records were grouped into three periods, 7.6–7.1 ka, 6.1–5.4 ka and 2 ka, thus improving the statistical significance of the number of El Niño events identified for each period. We then applied a coral $\delta^{18}\text{O}$ threshold analysis to assess which years in the records represent moderate to strong El Niños, in a fashion analogous to the Trenberth [1997] definition of an El Niño event, which is based on the post-1950 NINO3.4 Index (Figure 3). The average modern El Niño $\delta^{18}\text{O}$ anomaly for 1950–1997 was $0.18 \pm 0.06\text{‰}$ (1σ), relative to the 10-year running mean, and thus the $\delta^{18}\text{O}$ threshold for moderate El Niño events is defined as 0.12‰ (0.18‰ minus 1σ). Years with

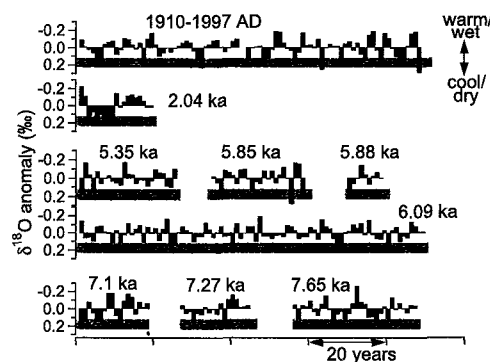


Figure 3. Comparison of interannual variability in modern and fossil annual coral $\delta^{18}\text{O}$ anomalies for the periods 7.6–7.1 ka, 6.1–5.4 ka and 2 ka. $\delta^{18}\text{O}$ anomalies were calculated relative to a 10-year running mean or, where <20 years were analysed, relative to the mean $\delta^{18}\text{O}$ value. Dashed lines at 0.18‰ indicate the average $\delta^{18}\text{O}$ anomaly recorded by modern coral MS01 for El Niños from 1950 to 1997. The dark grey box (0.12 – 0.24‰) indicates moderate El Niños (defined as $\pm 1\sigma$ from the average modern El Niño) and the light grey box (0.24 – 0.3‰) shows strong-very strong El Niños (defined as ± 1 – 2σ from the average modern El Niño).

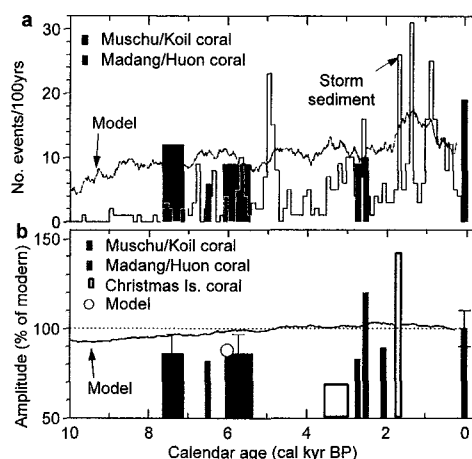


Figure 4. (a) Changes in El Niño frequency given by coral $\delta^{18}\text{O}$ records from Muschu Island, Koil Island, and Madang, PNG [Tudhope *et al.*, 2001], lacustrine storm deposits [Moy *et al.*, 2002], and model results [Clement *et al.*, 2000]. Data are scaled to events/century to facilitate direct comparison. (b) Changes in El Niño amplitude given by coral $\delta^{18}\text{O}$ records in panel A, the standard deviation of coral $\delta^{18}\text{O}$ in microatolls from Christmas Island, central equatorial Pacific [Woodroffe *et al.*, 2003], and model results [Clement *et al.*, 2000; Liu *et al.*, 2000]. The threshold amplitude analysis of the Tudhope *et al.* [2001] coral records is restricted to El Niño events to facilitate comparison with our records. Error bar for the modern MS01 coral record is the standard error of the mean for all El Niño events recorded for 1950–1997. Errors for fossil coral percentage changes include the standard errors for both the modern and fossil corals.

$\delta^{18}\text{O}$ values higher than 0.24‰ (0.18‰ plus 1–2 σ) are classed as strong to very strong El Niños.

4.1. El Niño Frequency

[10] Based on the $\delta^{18}\text{O}$ threshold analysis, the modern coral MS01 indicates an El Niño frequency of 19 events/century for 1950–1997, compared to 23 events/century given by the NINO3.4 Index for the same period. By contrast, the mid-Holocene coral $\delta^{18}\text{O}$ records show reduced El Niño frequencies of 12 and 8 events/century for the periods 7.6–7.1 ka and 6.1–5.4 ka, respectively (Figure 4a). The same threshold analysis of annually-averaged seasonal coral $\delta^{18}\text{O}$ data from Madang and Huon Peninsula, PNG also shows reduced El Niño frequency (6 events/century) at 6.5 ka, consistent with earlier interpretations of these data [Tudhope *et al.*, 2001]. The emerging picture of reduced El Niño frequency for the mid-Holocene western Pacific is consistent with the paleo-ENSO record from storm deposits in lake Laguna Pallcacocha, Ecuador [Rodbell *et al.*, 1999; Moy *et al.*, 2002], and recent model studies [Clement *et al.*, 2000; Liu *et al.*, 2000].

[11] Coupled ocean-atmosphere model studies of the Holocene suggest that El Niño variability has steadily increased from the mid-Holocene to the present [Clement *et al.*, 2000; Liu *et al.*, 2000]. Clement *et al.* [2000] attribute the lower mid-Holocene variability to precession of the Earth's equinoxes and the timing of equatorial ocean heating, such that equatorial Pacific trade winds strengthen

during the austral spring, providing a negative feedback on El Niño development. Liu *et al.* [2000] suggest that reduced El Niño intensity is caused by: (1) strengthening of the Asian summer monsoon and Pacific trade winds, and (2) weakening of the equatorial thermocline through subduction of warm southern subtropical water. While the coral evidence cannot resolve which model processes are causing the reduced El Niño frequency, they further confirm the model findings.

4.2. El Niño Amplitude

[12] We also estimated changes in El Niño amplitude from the annual coral $\delta^{18}\text{O}$ records. To facilitate comparison with modern events, El Niño amplitudes exceeding the moderate event threshold of 0.12‰ in $\delta^{18}\text{O}$ were averaged for each of the three Holocene periods (7.6–7.1 ka, 6.1–5.4 ka, 2 ka) and expressed as a percentage relative to the 1950–1997 event average (Figure 4b). In a similar way, paleo-El Niño amplitude was calculated for the nearby Tudhope *et al.* [2001] coral $\delta^{18}\text{O}$ records (6.5 ka, 2.7–2.5 ka). *Porites* microatoll $\delta^{18}\text{O}$ records from Christmas Island, central equatorial Pacific [Woodroffe *et al.*, 2003], were also included as a proxy for El Niño amplitude for the periods 3.7–2.7 ka and 1.7 ka.

[13] The coral $\delta^{18}\text{O}$ records show consistently reduced El Niño amplitude for the middle to late Holocene, except at 2.5–1.7 ka (Figure 4b). El Niño amplitude at Muschu Island is reduced to $85 \pm 12\%$ of modern values at 7.6–7.1 ka. The reduction in El Niño amplitude for the period 6.1–5.4 ka is the same (within error), while the Tudhope *et al.* [2001] record yields an average amplitude of 80% modern at 6.5 ka. El Niño amplitudes of 70–80% of modern are indicated for the period 3.7–2.7 ka. All records considered, the reduction in El Niño amplitude for the mid-Holocene is somewhat greater than the reduction to 90–95% of modern values given by the Clement *et al.* [2000] and Liu *et al.* [2000] models.

[14] All of the coral records for 2.5–1.7 ka reveal large and protracted $\delta^{18}\text{O}$ anomalies indicative of particularly severe El Niño events (Figure 5). The 2.5 ka Madang PNG coral records a protracted 4-year El Niño, like the 1991–1994 event, but almost twice the amplitude of 1997–

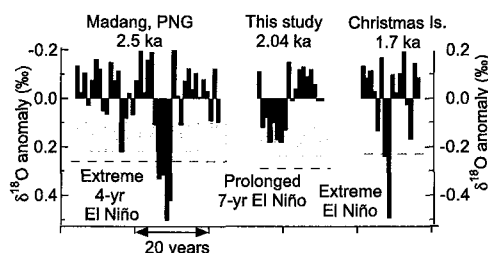


Figure 5. Comparison of extreme El Niño events recorded by tropical Pacific coral $\delta^{18}\text{O}$ records for the period 2.5–1.7 ka. The grey boxes indicate moderate El Niños ($\pm 1\sigma$ from the average modern El Niño) for this study and that of Tudhope *et al.* [2001]. Dashed lines indicate the magnitude of $\delta^{18}\text{O}$ anomalies recorded by Pacific corals during the very strong 1997–1998 El Niño. Negative $\delta^{18}\text{O}$ anomalies (warmer/wetter) are recorded by Christmas Island (central equatorial Pacific) *Porites* during El Niños [Woodroffe *et al.*, 2003].

1998 event [Tudhope *et al.*, 2001]. The 2 ka Muschu Island coral $\delta^{18}\text{O}$ record shows a severe 7-year El Niño, longer than any recorded Holocene or modern event. Moreover, the 1.7 ka *Porites* microatoll of Woodroffe *et al.* [2003] also records an extreme El Niño that was twice the amplitude of the 1997–1998 event. This is an interesting result as the three anomalously El Niño events are observed in an analysis spanning only ~ 70 years, which is much shorter than the modern instrumental record of ENSO. Given that these events are recorded by corals from widely separated Pacific locations, the results suggest that anomalous El Niño events may have been common during the period 2.5–1.7 ka. Moreover, the El Niño events recorded by the western and central equatorial Pacific corals for 2.5–1.7 ka exceed, by far, the modest ($\sim 5\%$) increase in El Niño amplitude given by models.

5. Model-Coral Proxy Discrepancies

[15] The model-proxy discrepancies for the mid-Holocene El Niño suppression and late Holocene amplification indicate a non-linear atmospheric response to El Niño SST changes. The PNG coral $\delta^{18}\text{O}$ clearly records El Niño-induced changes in both SST and rainfall amount ($\delta^{18}\text{O}_w$) in the equatorial western Pacific (Figure 1). If the atmosphere simply responded linearly to changes in El Niño SST forcing, then the percentage change in event amplitude (relative to modern) should be the same for the models and corals. This is clearly not the case.

[16] Strong El Niño precipitation anomalies in the central equatorial Pacific at ~ 2 ka have been attributed to tighter coupling between the Southern Oscillation and the Intertropical Convergence Zone (ITCZ) [Woodroffe *et al.*, 2003], which appears to have migrated southwards during the last $\sim 7,000$ years. The freshening of Warm Pool surface water since the mid-Holocene, as indicated by coupled measurements of Mg/Ca and $\delta^{18}\text{O}$ in surface-dwelling foraminifera [Stott *et al.*, 2002], and Sr/Ca and $\delta^{18}\text{O}$ in corals [Gagan *et al.*, 1998; McGregor, 2003], could also be related to a late Holocene increase in ITCZ precipitation. The late Holocene freshening and resulting increase in the buoyancy of the Warm Pool could have facilitated the eastward migration of warm surface waters triggered by westerly wind bursts, as occurs during strong El Niño events today [McPhaden, 1999; Picaut *et al.*, 2002]. The likelihood of westerly wind anomalies should have been at a maximum at ~ 2 ka because precession of the Earth's equinoxes was such that equatorial ocean heating opposed the development of SST gradients driving the Pacific trade winds during austral spring, thus allowing El Niño events to develop.

[17] Our results show that the ENSO system has the potential for more extreme variability than that observed in the modern instrumental record. The reduced El Niño frequency and amplitude during the mid-Holocene, and a shift to strong El Niño events at ~ 2.5 –1.7 ka, is similar to the pattern observed in modeling and paleo-lake studies. However, the coral records for ~ 2.5 –1.7 ka show evidence for El Niño events more severe than the 1997–1998 event, and longer than the multi-year 1991–1994 event. Therefore,

while our results indicate that model studies have captured the main processes controlling the evolution of the Holocene El Niño, clearly other processes must be considered to explain the non-linear response of the coupled ocean-atmosphere system.

[18] **Acknowledgments.** We thank G. Brunsell, I. Zagorskis, J. True and the crew of the rv Lady Basten for facilitating our participation in Project TROPICS. We also thank M. McCulloch, G. Mortimer, E-K. Potter, J. Cali and H. Scott-Gagan for analytical assistance, and T. Felis and H. Kuhnert for constructive comments on the manuscript.

References

- Ayliffe, L. K., M. I. Bird, M. K. Gagan *et al.* (2004), Geochemistry of coral from Papua New Guinea as a proxy for ENSO ocean-atmosphere interactions in the Pacific Warm Pool, *Cont. Shelf Res.*, in press.
- Clement, A. C., R. Seager, and M. A. Cane (2000), Suppression of El Niño during the mid-Holocene by changes in the Earth's orbit, *Paleoceanography*, 15, 731–737.
- Gagan, M. K., L. K. Ayliffe, D. Hopley *et al.* (1998), Temperature and surface-ocean water balance of the mid-Holocene tropical western Pacific, *Science*, 279, 1014–1018.
- Gagan, M. K., E. J. Hendy, S. G. Haberle, and W. S. Hantoro (2004), Post-glacial evolution of the Indo-Pacific Warm Pool and El Niño-Southern Oscillation, *Quat. Int.*, 118–119, 127–143.
- Liu, Z., J. Kutzbach, and L. Wu (2000), Modeling climate shift of El Niño variability in the Holocene, *Geophys. Res. Lett.*, 27, 2265–2268.
- McGregor, H. V. (2003), Coral reconstructions of mid-Holocene ocean-atmosphere variability in the Western Pacific Warm Pool, Ph.D. thesis, Aust. Nat. Univ., Canberra.
- McGregor, H. V., and M. K. Gagan (2003), Diagenesis and geochemistry of *Porites* corals from Papua New Guinea: Implications for paleoclimate reconstruction, *Geochim. Cosmochim. Acta*, 67, 2147–2156.
- McPhaden, M. J. (1999), Genesis and evolution of the 1997–98 El Niño, *Science*, 283, 950–954.
- McPhaden, M. J., and J. Picaut (1990), El Niño–Southern Oscillation displacements of the western equatorial Pacific warm pool, *Science*, 250, 1385–1388.
- Moy, C. M., G. O. Seltzer, D. T. Rodbell, and D. M. Anderson (2002), Variability of El Niño/Southern Oscillation activity at millennial time-scales during the Holocene epoch, *Nature*, 420, 162–165.
- Picaut, J., E. Hackert, A. J. Busalacchi *et al.* (2002), Mechanisms of the 1997–1998 El Niño–La Niña, as inferred from space-based observations, *J. Geophys. Res.*, 107(C5), 3037, doi:10.1029/2001JC000850.
- Rodbell, D. T., G. O. Seltzer, D. M. Anderson *et al.* (1999), An $\sim 15,000$ -year record of El Niño–driven alluviation in southwestern Ecuador, *Science*, 283, 516–520.
- Sandweiss, D. H., K. A. Maasch, R. L. Burger *et al.* (2001), Variation in Holocene El Niño frequencies: Climate records and cultural consequences in ancient Peru, *Geology*, 29, 603–606.
- Shulmeister, J., and B. G. Lees (1995), Pollen evidence from tropical Australia for the onset of an ENSO-dominated climate at c. 4000 BP, *Holocene*, 5, 10–18.
- Stott, L., C. Poulsen, S. Lund, and R. Thurnell (2002), Super ENSO and global climate oscillations at millennial time scales, *Science*, 297, 222–225.
- Tourey, Y. M., and W. B. White (1997), Evolution of the ENSO signal over the Indo-Pacific domain, *J. Phys. Oceanogr.*, 27, 683–696.
- Trenberth, K. E. (1997), The definition of El Niño, *Bull. Am. Meteorol. Soc.*, 78, 2771–2777.
- Tudhope, A. W., C. P. Chilcott, M. T. McCulloch *et al.* (2001), Variability in the El Niño–Southern Oscillation through a glacial-interglacial cycle, *Science*, 291, 1511–1517.
- Woodroffe, C. D., M. R. Beech, and M. K. Gagan (2003), Mid-late Holocene El Niño variability in the equatorial Pacific from coral microatolls, *Geophys. Res. Lett.*, 30(7), 1358, doi:10.1029/2002GL015868.

H. V. McGregor, Universität Bremen, FB5, Geowissenschaften, Postfach 330440, D-28334 Bremen, Germany. (mcgregor@uni-bremen.de)

M. K. Gagan, Research School of Earth Sciences, The Australian National University, Canberra, ACT 0200, Australia.